

Average-Value Model of Claw Pole Motor Drive for HIL Simulation of Integrated Starter Generator with Torque Assist for Mild Hybrid Application

Vinay Ranganath, Nitin Bhiwapurkar, and Govindarajan Srinivasan
Advanced Engineering, ERC, Tata Motors Limited, Pune, India, email: p.vinay@tatamotors.com

Abstract

For a low cost mild hybrid application, the integrated starter generator (ISG) is also used to provide torque assist to the engine. The claw pole type generator is widely used in automotive applications in belt-driven structures, where robustness and high speed operations are imposed. To understand the capability of claw pole machine for starter-generator and torque assist application, it needs to be modeled, simulated and tested in Hardware-in-the-loop (HIL). This paper describes the average-value modeling of claw pole motor-inverter systems, which is relatively challenging when the commutation period of inverter switches is also considered along with conduction period. The proposed average-value model appropriately includes both the commutation and conduction sub-intervals of inverter switches in 120° conduction mode. By avoiding the computation of switching events in power electronic models, the processing time of multi domain simulators can be decreased significantly. In this paper, the switched and the average-value models of claw pole motor-inverter system are developed and are simulated using MATLAB/ Simulink at sampling frequencies of 1 MHz and 10 kHz respectively. The results in both the cases are plotted and compared. HIL simulation is performed with the average-value model executed on DS1005 processor board using DS2211 I/O board and the ISG drive controller to validate the proposed average-value model.

Keywords: motor, hardware-in-the-loop (HIL), HEV (hybrid electric vehicle), inverter, modeling

1 Introduction

1.1 The mild hybrid system

The concept of using a single AC machine, as both starter and a generator, in an integrated starter generator (ISG) system has become popular and appears particularly attractive in automotive applications as it improves fuel efficiency of the vehicle with a small increment in cost [3]. In a mild hybrid application, the ISG system acts as the starter to crank the engine and

also provides torque assist to it when the vehicle accelerates. It acts as the generator to charge the battery when it doesn't operate in motoring mode. This mild hybrid system using an ISG can be adapted to conventional engine vehicles with only minimal system changes. The structure of a belt driven ISG system is presented in Fig.1. The popularity of claw-pole construction of electric machine for ISG application is mainly due to the high pole pair number which increases the torque density and robust structure allowing for high speed operation [2]. The machine is equipped with rotor winding supplied by the slip rings. The

machine is to be driven in a conventional manner that is similar to a conventional generator by a belt connected to the engine.

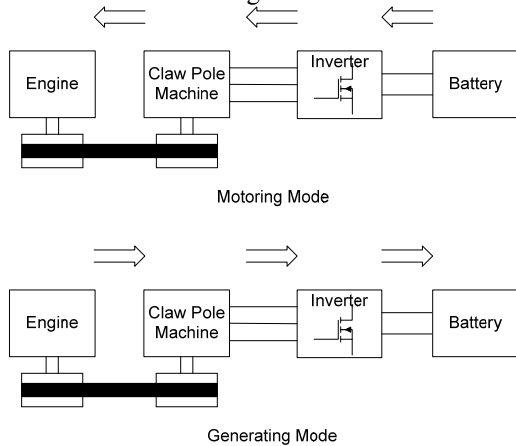


Figure1: Belt driven ISG system

1.2 Average-value model for HIL simulation

Hardware-in-the loop simulations are required to understand the capability of claw pole machine for torque assist application in the vehicle. The motor-inverter system can be simulated using a detailed switched model or an average-value model. For the efficient utilization of multi-domain simulation software, it is of high importance to have fast simulation models of power electronic components on hand. Especially in simulations of vast and complex electromechanical systems like that of a mild hybrid system, it is crucial to limit the processing effort to a minimum. Many times such electromechanical systems contain power electronic subsystems such as rectifiers, inverters, dc-dc converters etc. When simulating the power electronic devices with other electric and mechanical components of the application, computing the quantities of the power electronic models require a large share of the available processing power if switching events are calculated in the power electronic models. For a switched model of motor with a switching frequency of 10 kHz, the model has to be sampled at 200 kHz (considering a minimum duty ratio of 5%) to capture all the switching information. An average-value model requires only the duty cycle information of the PWM signals to model the inverter and hence a lower sampling frequency of the order of switching frequency (10 kHz) can be used. This saves lot of processing power of the processor and simulation

time is also reduced. In the average-value model, the effect of switching transients are neglected or averaged with respect to the switching interval which is of not much importance in a mild hybrid system as the torque ripple because of switching is averaged by the inertia of motor and engine. However, the switched model may be required in applications where switching transients and their effects are of much importance as in the case of simulating motor fault conditions like single phase to ground fault, three phase fault, device faults like MOSFET shoot-through etc.

2 Claw pole motor control

The drive schematic for claw-pole type motor is shown in Fig.2. Star configuration of the motor is considered. The control is similar to the BLDC motor control with the inverter operating in 120° conduction mode.

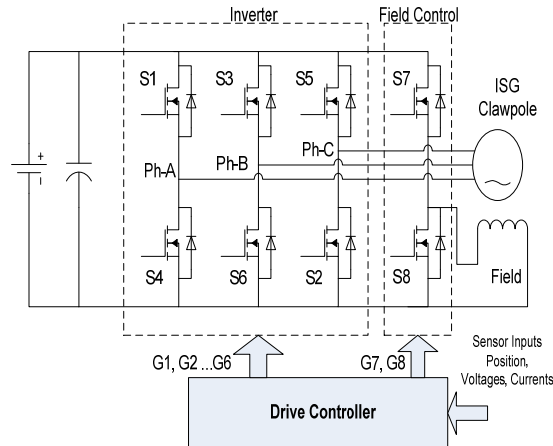


Figure2: Drive system for claw pole motor

Hall sensors A, B and C are used to detect the rotor position. Switching signals are generated based on the hall sensor feedback from the motor. Each switching sequence has one of the windings energized to positive power (current enters into the winding), the second winding is negative (current exits the winding) and the third is in a non-energized condition. Torque is produced because of the interaction between the magnetic field generated by the stator coils and the rotor coils. In order to keep the motor running, the magnetic field produced by the windings should shift position, as the rotor moves to catch up with the stator field.

Table1 shows the switching sequence that should be followed with respect to the Hall sensor feedback. Feedback signals such as currents and voltages are acquired by the controller and the motor torque is controlled by controlling the PWM duty of inverter switches so as to control the phase

$$i_a R + L \frac{di_a}{dt} = i_b R + L \frac{di_b}{dt} + V_{DC} + e_b - e_a \quad (11)$$

From equation (5),

$$i_b R + L \frac{di_b}{dt} = i_c R + L \frac{di_c}{dt} - V_{DC} + e_c - e_b \quad (12)$$

From equation (6),

$$i_c R + L \frac{di_c}{dt} = i_a R + L \frac{di_a}{dt} + e_a - e_c \quad (13)$$

Substituting (9) in (11),

$$2(i_a R + L \frac{di_a}{dt}) = -i_c R - L \frac{di_c}{dt} + V_{DC} + e_b - e_a \quad (14)$$

Substituting (13) in (14) and solving, the equation for phase 'a' current is obtained as:

$$\frac{di_a}{dt} + \frac{R}{L} i_a = \frac{V_{DC} + e_b - 2e_a + e_c}{3L} \quad (15)$$

Substituting (10) in (12),

$$2(i_b R + L \frac{di_b}{dt}) = -i_a R - L \frac{di_a}{dt} - V_{DC} + e_c - e_b \quad (16)$$

Substituting (11) in (16) and solving, the equation for phase 'b' current is obtained as:

$$\frac{di_b}{dt} + \frac{R}{L} i_b = \frac{-2V_{DC} - 2e_b + e_a + e_c}{3L} \quad (17)$$

Substituting (8) in (13),

$$2(i_c R + L \frac{di_c}{dt}) = -i_b R - L \frac{di_b}{dt} + e_a - e_c \quad (18)$$

Substituting (12) in (18) and solving, the equation for phase 'c' current is obtained as:

$$\frac{di_c}{dt} + \frac{R}{L} i_c = \frac{V_{DC} + e_a + e_b - 2e_c}{3L} \quad (19)$$

4.1.2 After Commutation of S_2

Current in phase 'c' becomes zero after the commutation of switch S_2 .

$$i_c = 0;$$

$$\frac{di_c}{dt} = 0 \quad (20)$$

The line-line voltage V_{AB} is given by

$$V_{AB} = V_{DC} = i_a R + L \frac{di_a}{dt} + e_a - e_b - L \frac{di_b}{dt} - i_b R \quad (21)$$

From (21),

$$i_a R + L \frac{di_a}{dt} = i_b R + L \frac{di_b}{dt} + V_{DC} + e_b - e_a \quad (22)$$

We have,

$$i_a = -i_b;$$

Substituting in (22), the phase 'a' current after commutation of S_2 is obtained as:

$$\frac{di_a}{dt} + \frac{R}{L} i_a = \frac{V_{DC} - e_a + e_b}{2L} \quad (23)$$

4.2 Case 2:

4.2.1 During Commutation of S_1 :

Considering switches 5, 6 & 1 as shown in Fig.2 as the switches coming into conduction, staying in conduction and going out of conduction respectively, the line-line terminal voltages of the machine are given by:

$$V_{AB} = 0 = i_a R + L \frac{di_a}{dt} + e_a - e_b - L \frac{di_b}{dt} - i_b R \quad (24)$$

$$V_{BC} = -V_{DC} = i_b R + L \frac{di_b}{dt} + e_b - e_c - L \frac{di_c}{dt} - i_c R \quad (25)$$

$$V_{CA} = V_{DC} = i_c R + L \frac{di_c}{dt} + e_c - e_a - L \frac{di_a}{dt} - i_a R \quad (26)$$

From (24),

$$i_a R + L \frac{di_a}{dt} = i_b R + L \frac{di_b}{dt} + e_b - e_a \quad (27)$$

From (25),

$$i_b R + L \frac{di_b}{dt} = i_c R + L \frac{di_c}{dt} - V_{DC} + e_c - e_b \quad (28)$$

$$i_c R + L \frac{di_c}{dt} = i_a R + L \frac{di_a}{dt} + e_a - e_c + V_{DC} \quad (29)$$

Substituting (9) in (27)

$$2(i_a R + L \frac{di_a}{dt}) = -i_c R - L \frac{di_c}{dt} + e_b - e_a \quad (30)$$

Substituting (29) in (30) and solving, the equation for phase 'a' current is obtained as:

$$\frac{di_a}{dt} + \frac{R}{L} i_a = \frac{-V_{DC} - 2e_a + e_b + e_c}{3L} \quad (31)$$

Substituting (10) in (28),

$$2(i_b R + L \frac{di_b}{dt}) = -i_a R - L \frac{di_a}{dt} - V_{DC} + e_c - e_b \quad (32)$$

Substituting (27) in (32) and solving, the equation for phase 'b' current is obtained as:

$$\frac{di_b}{dt} + \frac{R}{L} i_b = \frac{-V_{DC} + e_a - 2e_b + e_c}{3L} \quad (33)$$

Substituting (8) in (29),

$$2(i_c R + L \frac{di_c}{dt}) = -i_b R - L \frac{di_b}{dt} + e_a - e_c + V_{DC} \quad (34)$$

Substituting (28) in (34) and solving, the equation for phase 'c' current is obtained as:

$$\frac{di_c}{dt} + \frac{R}{L} i_c = \frac{2V_{DC} + e_a + e_b - 2e_c}{3L} \quad (35)$$

4.2.2 After Commutation of S_1 :

Current in phase 'a' becomes zero after the commutation of switch S_1 .

$$i_a = 0;$$

$$\frac{di_a}{dt} = 0;$$

The line-line voltage V_{BC} is given by:

$$V_{BC} = -V_{DC} = i_b R + L \frac{di_b}{dt} + e_b - e_c - L \frac{di_c}{dt} - i_c R \quad (36)$$

We have,

$$i_c = -i_b;$$

Substituting in (33), the phase 'b' current after commutation of S_1 is obtained as:

$$\frac{di_b}{dt} + \frac{R}{L} i_b = \frac{-V_{DC} - e_b + e_c}{2L} \quad (37)$$

From equations (15),(17),(19),(23),(31),(33),(35) and (37), it can be generalized for PWM signals of duty ratio D that if Y is the outgoing phase, X is the incoming phase and W is the phase staying in conduction,

For the commutation of upper phase

Before commutation, the equations for phase currents are given by:

$$\frac{di_Y}{dt} + \frac{R}{L} i_Y = \frac{-DV_{DC} - 2e_Y + e_W + e_X}{3L} \quad (38)$$

$$\frac{di_W}{dt} + \frac{R}{L} i_W = \frac{-DV_{DC} + e_Y - 2e_W + e_X}{3L} \quad (39)$$

$$\frac{di_X}{dt} + \frac{R}{L} i_X = \frac{2DV_{DC} + e_Y + e_W - 2e_X}{3L} \quad (40)$$

After commutation, the equations for phase currents are given by:

$$\frac{di_W}{dt} + \frac{R}{L} i_W = \frac{-DV_{DC} - e_W + e_X}{2L}; \quad (41)$$

$$i_X = -i_W \quad (42)$$

$$i_Y = 0 \quad (43)$$

For the commutation of lower phase

Before commutation, the equations for phase currents are given by:

$$\frac{di_Y}{dt} + \frac{R}{L} i_Y = \frac{DV_{DC} - 2e_Y + e_W + e_X}{3L} \quad (44)$$

$$\frac{di_W}{dt} + \frac{R}{L} i_W = \frac{DV_{DC} + e_Y - 2e_W + e_X}{3L} \quad (45)$$

$$\frac{di_X}{dt} + \frac{R}{L} i_X = \frac{-2DV_{DC} + e_Y + e_W - 2e_X}{3L} \quad (46)$$

After commutation, the equations for phase currents are given by:

$$\frac{di_W}{dt} + \frac{R}{L} i_W = \frac{DV_{DC} - e_W + e_X}{2L} \quad (47)$$

$$i_X = -i_W \quad (48)$$

$$i_Y = 0 \quad (49)$$

The other equations such as the motor torque, rotor angle, etc. are same as described in the switched model section.

Table2: Parameters of the motor-inverter system used

Battery open circuit voltage	48 V
Battery internal resistance	32 mΩ
DC bus capacitance	10000 μF
Machine inductance (per phase)	56.25 μH
Machine resistance (per phase)	11.5 mΩ
Machine constant	0.086 V·s/rad
Number of poles	12
Engine inertia	0.12 Kg·m ²

5 Comparison of switched and average-value models

The ISG system is operated in a constant speed mode with the ISG drive unit controlling the duty cycle of inverter switches. Parameters of the motor-inverter system used are shown in Table 2. The results obtained from the switched and average-value models at different operating points are shown below:

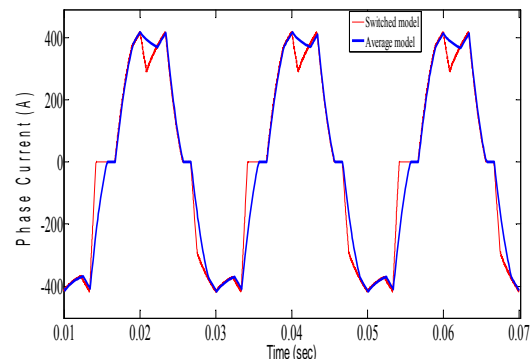


Figure4: Phase current at 500 rpm and 50% PWM duty

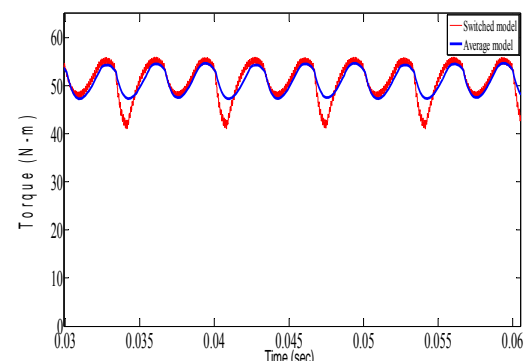


Figure5: Torque at 500 rpm and 50% PWM duty

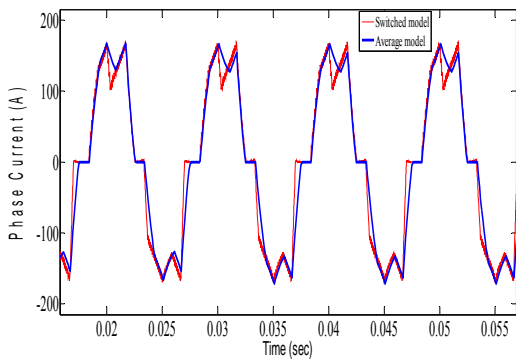


Figure6: Phase current at 1000 rpm and 50% PWM duty

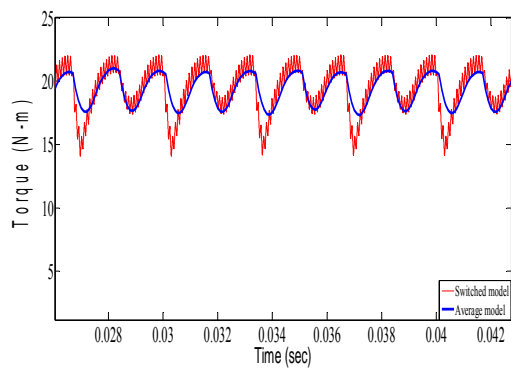


Figure7: Torque at 1000 rpm and 50 % PWM duty

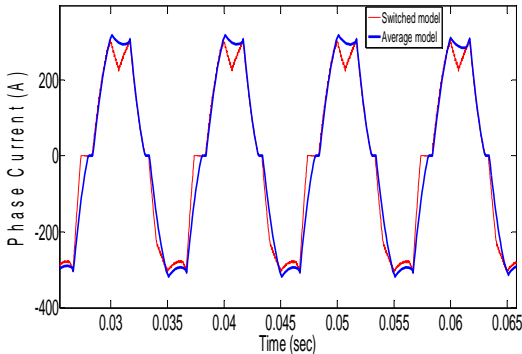


Figure8: Phase current at 1000 rpm and 70% PWM duty

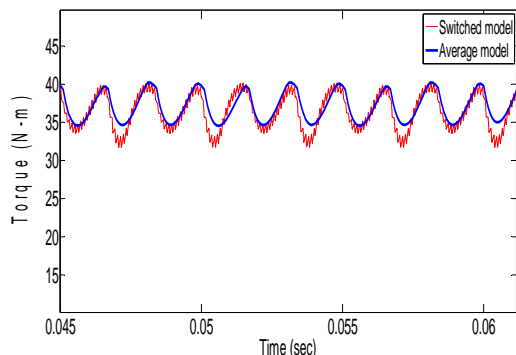


Figure9: Torque at 1000 rpm and 70% PWM duty

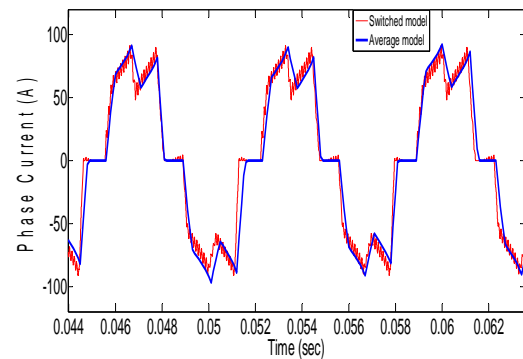


Figure10: Phase current at 1500 rpm and 60 % PWM duty

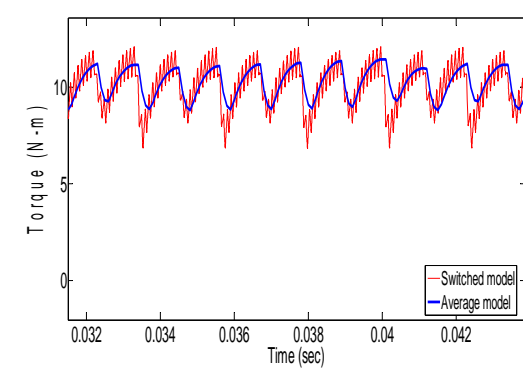


Figure11: Torque at 1500 rpm and 60 % PWM duty

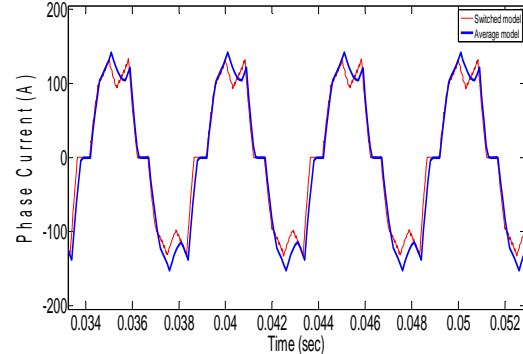


Figure12: Phase current at 2000 rpm and 90% PWM duty

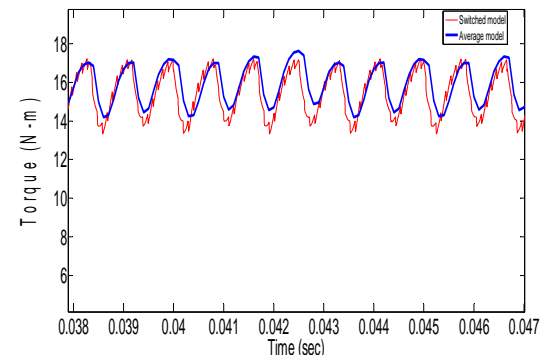


Figure13: Torque at 2000 rpm and 90 % PWM duty

It can be seen that the curves of the average-value model trace the average values of the curves of switched model. Some deviations are present during phase commutations which are negligible when average motor torque is considered.

6 HIL simulation of ISG using average-value model

The Block diagram of HIL (hardware-in-the-loop) system for ISG is shown in Fig.14. The claw pole motor-inverter system is implemented on dSPACE DS1005 processor board and DS2211 I/O board. The dSPACE system acts as the virtual motor-inverter and provides the real time interface to the ISG drive controller. The controller takes commands from vehicle-ECU and controls the ISG by generating appropriate PWM signals for inverter. The dSPACE model takes the PWM signals as input and outputs various sensor signals to the drive controller.

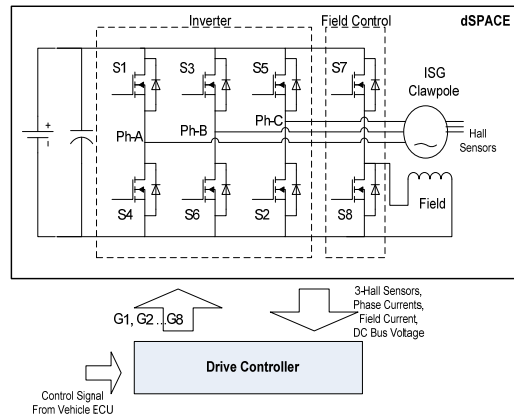


Figure14: Block diagram of HIL system

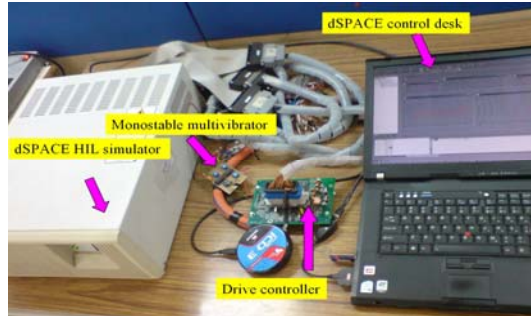


Figure15: HIL set-up

The HIL set-up used is shown in Fig.15. A sampling frequency of 10 kHz is used. A monostable multivibrator circuit is used to generate continuous “ON” signals whenever top

switches undergo PWM. dSPACE control desk is used for calibration and measurement.

The results of HIL simulation using average-value model and their comparison with the computer simulation of average-value model are shown in Fig.16 to 27. In HIL system, dSPACE updates the duty value of gate signals after the sample time of 100us. This introduces a delay of 100us in the gate signals. In computer simulation model a delay of 100us is introduced in the gate signals from controller block purposefully to simulate the behaviour of HIL system, so that the results can be compared with HIL system.

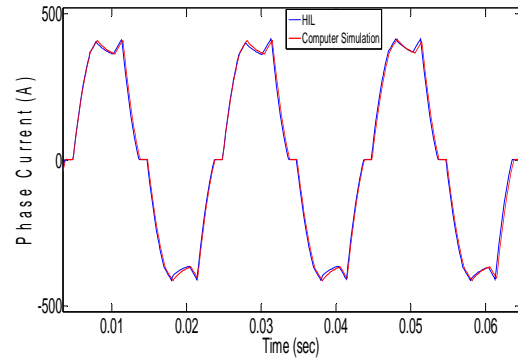


Figure16: Phase Current at 500 rpm and 50% PWM duty

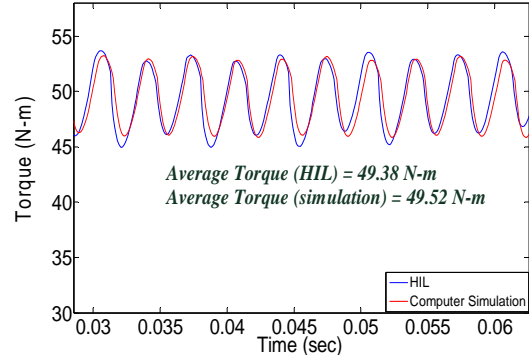


Figure17: Torque at 500 rpm and 50% PWM duty

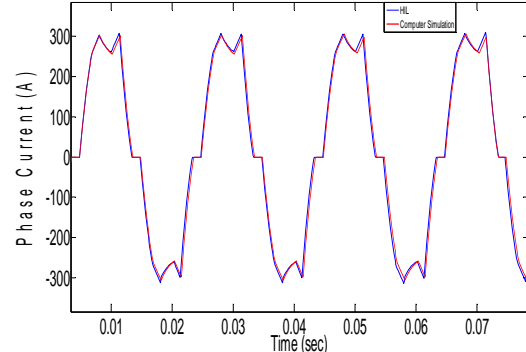


Figure18: Phase Current at 500 rpm and 40% PWM duty

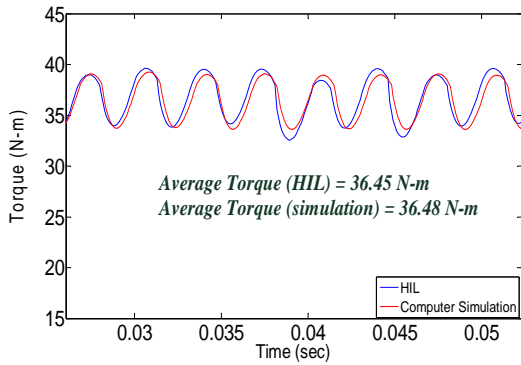


Figure19: Torque at 500 rpm and 40% PWM duty

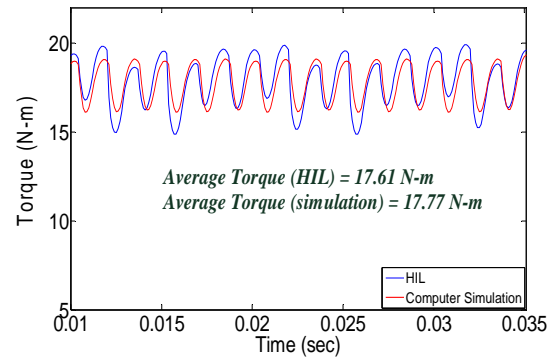


Figure23: Torque at 1000 rpm and 50% PWM duty

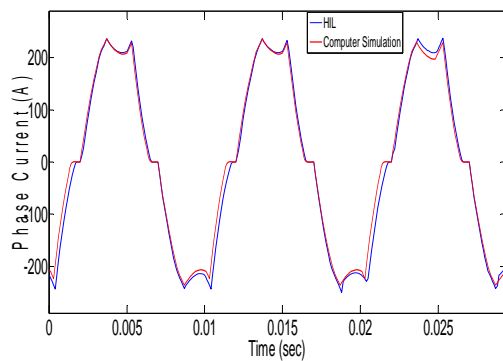


Figure20: Phase current at 1000 rpm and 60% PWM duty

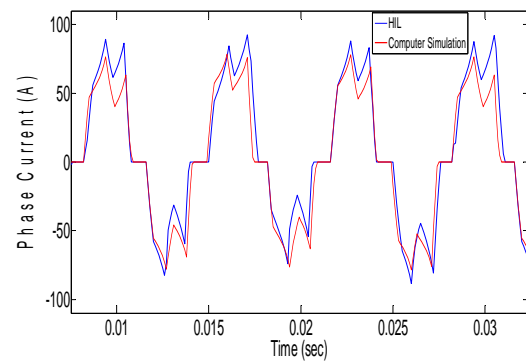


Figure24: Phase current at 1500 rpm and 60% PWM duty

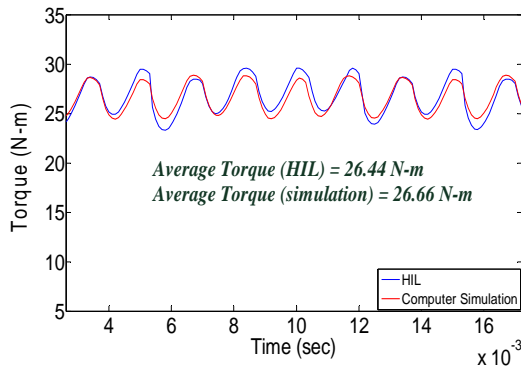


Figure21: Torque at 1000 rpm and 60% PWM duty

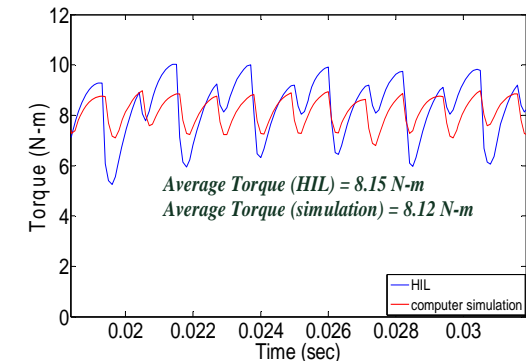


Figure25: Torque at 1500 rpm and 60% PWM duty

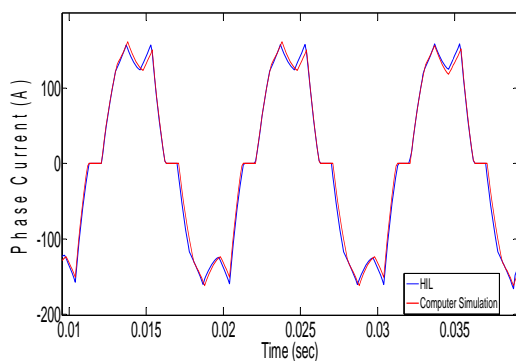


Figure22: Phase current at 1000 rpm and 50% PWM duty

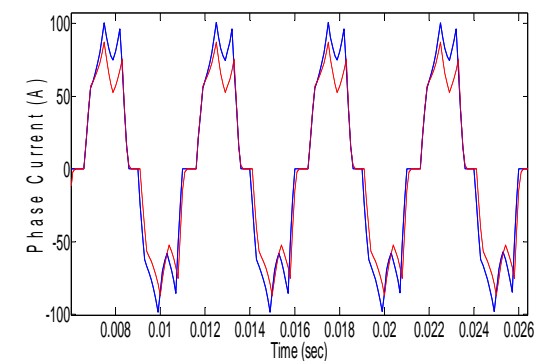


Figure26: Phase current at 2000 rpm and 80% PWM duty

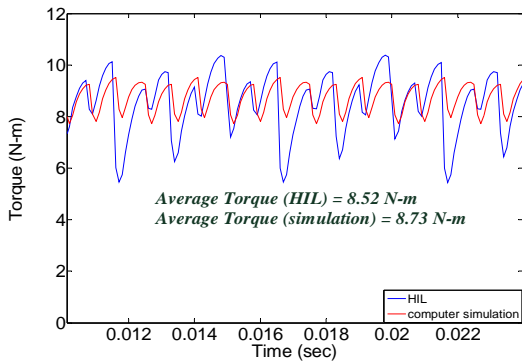


Figure27: Torque at 2000 rpm and 80% PWM duty

It can be seen that the average torque in HIL testing and computer simulation of average-value model are almost same. Small difference in the value of average torque is due to one-sample inaccuracy of dSPACE PWM measurement blocks and the delay introduced by monostable multivibrator circuit.

7 Conclusions

As the switched model of claw pole machine for HIL application requires high sampling frequency to capture the duty range of PWM signals, the average-value model is developed which can be sampled at lower frequency as switching information is not required. The results of average-value and switched models are compared and it is observed that they are in mutual agreement with each other. The discussed average-value model can be implemented in existing dSPACE hardware (DS1005), saving potential cost of hardware upgradation required for the implementation of switched model.

References

- [1] Ali Emadi, *Handbook of Automotive Power Electronics and Motor Drives*, CRC Press, 2005.
- [2] Geun-Ho Lee, Geo-Seung Choi, and Woongchul Choi, *Design Considerations for Low Voltage Claw Pole Type Integrated Starter Generator (ISG) Systems*, Journal of Power Electronics (JPE), Vol. 11, No.4, 2011.
- [3] J. E. Walters and R. J. Krefta, *Technology Considerations for Belt Alternator Starter Systems*, SAE World Congress, Mar. 2004.
- [4] *Hardware Installation and Configuration Reference*, dSPACE, Release 7.0, Nov.2010.

Authors

Vinay Ranganath was born in Andhra Pradesh, India, in 1985. He received his M.Tech. in Power and Control from IIT Kanpur, India in 2009, and his B.E. in Electrical Engineering from Osmania University, Hyderabad, India in 2006. Since 2009, he is with Tata Motors Limited, Pune, India. His current research interests include advanced control of electric machines, Power electronic converters, electric and hybrid electric vehicles.



Nitin Bhiwapurkar received his Ph.D. in Electrical Engg. from Univ. of Minnesota, Minneapolis, USA in 2006, M.Tech. in Power Electronics and Power Systems from IIT Bombay, India in 2000 and B.E. in Electrical Engineering from Regional College of Engineering, (VNIT) Nagpur, India in 1997. Presently he is working in Tata Motors Ltd, India in Advanced Engineering Department, ERC. His research interests include electric machine drives, Power electronic converters, hybrid & electric vehicles (HEVs) and embedded control application in HEVs.



Govindarajan Srinivasan was born in Devakottai, India in 1955. He received his B.Tech. in Electrical Engineering from Indian Institute of Technology, Madras (Chennai). He is heading the department of Advanced Engineering in Tata Motors Ltd, Pune, India and is currently responsible for projects in hybrid / electric and fuel cell vehicles. He is a strong supporter to adopt methods of mathematical modeling & simulation to arrive at the optimum solutions and to reduce development time. He takes keen interest to guide young engineers to apply scientific knowledge to find innovative solutions.

